HHS Public Access

Author manuscript

*J Ultrasound Med*. Author manuscript; available in PMC 2015 June 05.

Published in final edited form as:

*J Ultrasound Med*. 2014 August ; 33(8): 1417–1426. doi:10.7863/ultra.33.8.1417.

# Acoustic Radiation Force for Noninvasive Evaluation of Corneal Biomechanical Changes Induced by Cross-linking Therapy

**Raksha Urs, PhD**, **Harriet O. Lloyd, MS**, and **Ronald H. Silverman, PhD**

Department of Ophthalmology, Columbia University Medical Center, New York, New York USA (R.U., H.O.L., R.H.S.); and Frederic L. Lizzi Center for Biomedical Engineering, Riverside Research Institute, New York, New York USA (R.H.S.)

## Abstract

**Objectives—**To noninvasively measure changes in corneal biomechanical properties induced by ultraviolet-activated riboflavin cross-linking therapy using acoustic radiation force (ARF).

**Methods—**Cross-linking was performed on the right eyes of 6 rabbits, with the left eyes serving as controls. Acoustic radiation force was used to assess corneal stiffness before treatment and weekly for 4 weeks after treatment. Acoustic power levels were within US Food and Drug Administration guidelines for ophthalmic safety. Strain, determined from ARF-induced displacement of the front and back surfaces of the cornea, was fit to the Kelvin-Voigt model to determine the elastic modulus ($E$) and coefficient of viscosity ($\eta$). The stiffness factor, the ratio of $E$ after treatment to $E$ before treatment, was calculated for treated and control eyes. At the end of 4 weeks, ex vivo thermal shrinkage temperature analysis was performed for comparison with in vivo stiffness measurements. One-way analysis of variance and Student $t$ tests were performed to test for differences in $E$, $\eta$, the stiffness factor, and corneal thickness.

**Results—**Biomechanical stiffening was immediately evident in cross-linking–treated corneas. At 4 weeks after treatment, treated corneas were 1.3 times stiffer and showed significant changes in $E$($P$= .006) and $\eta$ ($P$= .007), with no significant effect in controls. Corneal thickness increased immediately after treatment but did not differ significantly from the pretreatment value at 4 weeks.

**Conclusions—**Our findings demonstrate a statistically significant increase in stiffness in cross-linking–treated rabbit corneas based on in vivo axial stress/strain measurements obtained using ARF. The capacity to noninvasively monitor corneal stiffness offers the potential for clinical monitoring of cross-linking therapy.

### Keywords

acoustic radiation force; cornea; cross-linking; elasticity; keratoconus; ultrasound

Keratoconus is a progressive, noninflammatory form of corneal dystrophy resulting from the biomechanical weakening and destabilization of the cornea. It is characterized by thinning and bulging of the corneal stroma, which causes deterioration in vision.[1] The incidence of



Address correspondence to Raksha Urs, PhD, Department of Ophthalmology, Columbia University Medical Center, 160 Fort Washington Ave, Room 711C, New York, NY 10032 USA. ru2118@columbia.edu.

this disease is 1 per 2000, and it manifests primarily in young adults. The clinically approved treatments available in the United States (contact lenses and corneal inserts) are aimed at improvement of visual function. Although these treatment options temporarily ameliorate the symptoms of deteriorating vision, they do not address corneal destabilization, which is the basis of the disease. Disease progression may ultimately necessitate corneal transplantation to preserve vision.

Corneal cross-linking therapy has emerged as a treatment option for keratoconus.[2–4] In cross-linking, riboflavin and ultraviolet light are used to induce photosensitized oxidation to augment the collagen bonds in the weakened corneal stroma. This procedure strengthens the cornea and interrupts the process of biomechanical failure. Cross-linking therapy is practiced in Europe and several other countries and is undergoing clinical trials in the United States for approval by the Food and Drug Administration. It continues to evolve with the development of new cross-linking agents[5] and methods to minimize patient discomfort.[6,7]

Various measurement parameters have been used to establish the stiffening effect of cross-linking therapy. Histologic evaluation has revealed substantial increases in the stromal collagen fiber diameter.[8] An increased corneal shrinkage temperature[9] and resistance to collagen-digesting enzymes[10] are also indicative of improved biomechanical stability. A variety of ex vivo biomechanical tests have also been conducted to show post-cross-linking improvement in the biomechanical properties of the cornea.[11] Excised tissue has been biomechanically analyzed using microcomputer-controlled biomaterial-testing devices,[12–14] gel electrophoresis,[15] eye inflation testing,[16] supersonic shear wave imaging,[17] atomic force microscopy,[18] and Brillouin microscopy.[19] Ex vivo studies have found that the cross-linked cornea is stiffer than the normal cornea by factors of 1.6 in rabbit corneas[20] and 1.8 and 4.5 in porcine and human corneas,[13] respectively. However, as there is a paucity of methods to evaluate corneal biomechanical properties noninvasively, improvement in corneal stiffness has not been verified in vivo. The clinical outcome of cross-linking therapy is currently assessed with functional and structural measurements, such as manual keratometry, uncorrected and best spectacle–corrected visual acuity, manifest refraction, pachymetry, topography, intraocular pressure, and slit lamp examinations.[21,22] Typically, patients are examined once every 3 months after treatment for up to a year and once per year thereafter. Therefore, disease progression, which is the marker of treatment failure, might not be evident for months or years. Because such progression may result in irreparable damage to the cornea, there is an urgent need to develop a clinically applicable means to assess cross-linking–induced changes in corneal biomechanical properties noninvasively.

Currently, no clinical device is capable of directly measuring post–cross-linking biomechanical changes in corneal tissue. The sole clinical tool at this time is the Ocular Response Analyzer (Reichert Technologies, Depew, NY).[23] This device produces deflection of the cornea in response to an air puff and records the air pressure when the cornea is flattened (applanated) as it indents and as it recovers. Hysteresis is calculated from the difference in the inward and outward pressure values obtained during the bidirectional applanation process and is presumed to result from viscous damping. Standard parameters available from the Ocular Response Analyzer have shown no difference between normal and cross-linked eyes.[24–26] The area under the second applanation pressure curve, a parameter

available from newer versions of the Ocular Response Analyzer software, appears to detect changes in the cross-linked eye, but additional studies are needed to find associations between this parameter and corneal biomechanical properties.[27] Of the many techniques that have been demonstrated on ex vivo tissue, supersonic shear wave imaging[17] and Brillouin microscopy[19] might be developed for in vivo use, but remain under investigation.

Acoustic radiation force (ARF) can be used to remotely generate localized stress and strain in tissue. Acoustic radiation force–induced stress is generated by transfer of momentum from an ultrasound beam to tissue through absorption and scattering. In soft tissues, most of the momentum transfer is through absorption. The axial displacement of tissue caused by this radiation force is a function of the magnitude of the applied force and tissue elasticity.[28–30]

There are numerous approaches to elasticity measurement using ARF,[31] such as acoustic streaming,[32] sonorheometry,[33] acoustic radiation force impulse imaging,[30] monitored steady-state excitation and recovery,[34] shear wave elasticity imaging,[35] supersonic shear imaging,[36] vibro-acoustography,[37] and harmonic motion imaging.[38] In acoustic radiation force impulse imaging, a short-duration ARF is applied with conventional pulse-echo transducers, and the on-axis displacements are measured with the same transducer.[30,39] Clinically, acoustic radiation force impulse imaging has been used to characterize a wide variety of soft tissue lesions such as those in the kidney[40] and liver.[41–43] Although ARF technology is available in some commercial linear array–based ultrasound systems (eg, Acuson S2000; Siemens Medical Solutions, Mountain View, CA), such systems are of limited value for evaluation of ocular tissues because of their relatively low resolution and lack of axial beam symmetry.

We have developed instrumentation and techniques based on the use of ARF and high-resolution ultrasound imaging to characterize ocular tissue safely and noninvasively. In our implementation, a single-element focused ultra-sound transducer is used both to generate ARF and to image ARF-induced displacements. We recently reported the effect of ARF on the in vivo rabbit choroid, the vascular layer of tissue supporting the retina.[44] In this report, we demonstrate the use of ARF in the in vivo evaluation of corneal stiffness changes induced by cross-linking.

## Materials and Methods

All experiments were performed in compliance with the Association for Research in Vision and Ophthalmology Statement for the Use of Animals in Ophthalmic and Vision Research under a research protocol approved by Columbia University Medical Center's Institutional Animal Care and Use Committee. New Zealand White rabbits (n = 6) were used in this study.

### Cross-linking Treatment

A standard cross-linking procedure was performed on the right eyes of the rabbits. The rabbits were placed under general anesthesia with intramuscular injection of xylazine (5 mg/kg) and ketamine (35 mg/kg). The corneal epithelium was treated with 20% ethanol for

60 seconds and then removed with a sharp beaver blade. Two drops of 0.1% riboflavin solution (10 mg of riboflavin-5-phosphate in 10 mL of dextran 20% solution) were applied to the cornea every 3 minutes for 30 minutes to allow sufficient saturation of the stroma. Then an 8-mm-diameter region of the central cornea was irradiated for 30 minutes with ultraviolet A light (Opto XLink corneal cross-linking system; Opto Electronica, Sao Carlos, Brazil) with a wavelength of 370 nm and irradiance of 3 $mW/cm^2$. During irradiation, instillation of riboflavin was continued at the rate of 2 drops every 3 minutes. The rabbits were provided with a prophylactic treatment of subcutaneous buprenorphine (0.05–0.1 mg/kg) before initiation of the procedure and every 12 hours thereafter for 72 hours for pain management.

## Ultrasound System

The ultrasound excitation system consisted of a programmable arbitrary waveform generator (WW1281A; Tabor Electronics, Tel Hanan, Israel), a 55-dB broadband radiofrequency amplifier (A150; Electronic Navigation Industries, Rochester, NY), and a diode expander circuit. The transducer (V324-SU; Panametrics, Waltham, MA) had a center frequency of 25 MHz, a 6-mm aperture, and an 18-mm focal length. Phase-resolved radiofrequency echo data returned through the diode expander circuit, a limiter, a preamplifier (AU1480; MITEQ, Inc, Hauppauge, NY), a 3-MHz high-pass filter, and a 30-MHz low-pass filter and were passed to a digitizer (Acqiris DP310; Agilent Technologies, Monroe, NY). Radiofrequency echo data were acquired at a sample rate of 400 MHz at 12-bit precision. Custom data acquisition software was implemented with LabView (National Instruments, Austin, TX). Transducer output was characterized with a certified 40-μm needle hydrophone calibrated up to 60 MHz (Precision Acoustics, Ltd, Higher Bockhampton, Dorchester, England).

## Acoustic Radiation Force Imaging Method

The ARF pulse-excitation sequence incorporates brief temporal gaps between force applications that allow acquisition of pulse-echo tracking data during the course of the push. Tracking pulses, emitted at a pulse repetition frequency of 2 kHz, consisted of 25-MHz monocycles. Pushing pulses were 400-microsecond, 25-MHz tone bursts. The ARF sequence consisted of a prepush mode, with 10 tracking pulses to establish baseline corneal anterior and posterior interface positions; a push mode, with 20 pushing pulses interleaved between tracking pulses (an 80% duty cycle); and a recovery mode, with 400 tracking pulses. The ARF sequence allowed determination of preexposure baseline conditions (including corneal thickness) and measurement of displacement with time of both corneal surfaces during the 8-millisecond push sequence and during recovery. The tracking and push pulses were generated using a 500 mV peak-to-peak amplitude before 55-dB amplification (280 V peak to peak).

For each eye, ARF data were acquired in triplicate at 3 points in the central 1.5 mm of the cornea, yielding 9 sets of data per imaging session. Assuming plane-wave propagation and that force is generated only by absorption, the magnitude of ARF, $F$ ($N/m^3$), was obtained from

$$F=\frac{2\alpha I}{c}, \quad (1)$$

where α is the attenuation coefficient of the cornea ($m^{-1}$); $I$ is the intensity ($W/cm^2$); and $c$ is the speed of sound in the cornea (m/s). The constant stress, σ (Pa), absorbed by the cornea was computed as

$$\sigma=FT, \quad (2)$$

where $T$ (m) is the thickness of the cornea.

## Image Acquisition

Rabbits were imaged under general anesthesia with intramuscular injection of xylazine (5 mg/kg) and ketamine (35 mg/kg). The eye was gently proptosed and placed through a hole in a latex membrane to form a watertight seal. The membrane was secured to a ring stand to form a normal saline water bath, which provided acoustic coupling between the ultrasound transducer and the eye. Acoustic radiation force examinations were performed on both the control (left) and treated (right) eyes. Baseline ARF examinations were made on the day before the right eyes were treated. After treatment, ARF examinations were made weekly for 4 weeks.

## Data Analysis

The radiofrequency data from the M-mode images were analyzed with custom software developed in MATLAB version 7.14 (The MathWorks, Natick, MA). Corneal thickness was measured in the prepush mode, assuming a corneal speed of sound of 1640 m/s. A spline-based algorithm[45] was used to track the continuous displacement of the front and back surfaces of the cornea to determine the observed temporal change in corneal thickness, $\Delta T(t)$, during the push and the relaxation modes. Continuous strain, $\varepsilon(t)$, was computed as

$$\varepsilon(t)=\frac{\Delta T(t)}{T}. \quad (3)$$

Average strain was determined at each of the 3 measurement positions in the central cornea, yielding 3 strain curves per rabbit. Acoustic radiation force–induced strain was fit to the viscoelastic Voigt model, using a nonlinear least squares optimization routine in MATLAB, where the best-fit parameters represent the in vivo material properties. The Voigt model describes the continuous deformation response of a viscoelastic material to a constant stress:

$$\varepsilon(t)=\alpha\left(1-e^{\frac{-t}{\tau}}\right), \quad (4)$$

where the constant $a = \sigma/E$, σ (Pa) being the magnitude of the constant stress and $E$ (Pa) the elastic modulus; $t$ (s) is time; and the time constant $\tau = \eta/E$, where η (Pa/s) is the coefficient of viscosity. Average $E$ and η were calculated for each eye. The stiffness factor, the ratio of $E$ after treatment to $E$ before treatment, was determined for each eye at each time point. One-way analysis of variance (ANOVA) was performed to test for temporal differences in $E$, ν, the stiffness factor, and thickness in the treatment and control groups. For the treated

eyes, the Student *t* test was performed to test for significant differences for all of these parameters from pretreatment values at 4 weeks after treatment.

### Ex Vivo Thermal Shrinkage Temperature Analysis

Thermal shrinkage temperature analysis can be used to assess corneal cross-linking in ex vivo tissue.[9] Progressive heating of collagen fibers causes disruption of hydrogen bonds in the collagen molecule triple helix at a critical threshold temperature, resulting in rapid tissue shrinkage.[46] The thermal shrinkage temperature can be expressed in various ways, including temperature of onset of tissue shrinkage,[47] temperature at the maximum change in tissue shrinkage,[48] and temperature at shrinkage to one-third of the initial length.[49] Here we assessed the temperature at shrinkage to one-third of the initial tissue area ($T_{⅓}$).

At the end of 4 weeks, rabbits were euthanized under general anesthesia with an overdose of intravenous sodium phenobarbital, and their corneas were extracted from enucleated eyes. Corneal strips of 2 × 6 mm were placed in a polyethylene box whose temperature was controlled by circulating heated water through the box.[46] A digital photo scanner (G4010; Hewlett-Packard, Palo Alto, CA) connected to a computer was used to record images as the temperature was raised from 50°C to 70°C at a rate of 1°C/min. The digital images were analyzed with ImageJ software (National Institutes of Health, Bethesda, MD), and the percent change in area was determined. The percent change in area–versus–temperature curves were fit to a Boltzmann sigmoidal function, and the $T_{⅓}$ was calculated from the best-fit curves. Differences in $T_{⅓}$ ($\Delta T_{⅓}$) between treated and control tissue were computed for each rabbit. These values were compared to stiffness factors.

## Results

Hydrophone measurements of the ultrasound beam in the focal plane showed a – 12-dB beam width of 285 μm, a peak negative pressure of 2.4 MPa, and a peak pulse average intensity of 161.5 W/cm$^2$ at the focus. The derated spatial-peak pulse-average intensity was 6.37 W/cm$^2$, and the mechanical index was 0.08. The derated spatial-peak temporal-average intensity measured 10.2 mW/cm$^2$ for ARF sequences spaced 5 seconds apart (the interval between successive exposures).

The cross-linking procedure was interrupted because of technical problems in 2 rabbits, which received only partial treatment. Assuming a constant corneal thickness of 385 μm for the rabbit cornea, an attenuation coefficient of 0.93 dB cm$^{-1}$ MHz$^{-1}$,[50] and a corneal speed of sound of 1640 m/s, the stress absorbed by the cornea due to ARF exposure was calculated from equations 1 and 2 to be 196.5 Pa.

Figure 1A shows a B-scan image of a rabbit cornea and the anterior surface of the lens. The horizontal line indicates the line of sight along which ARF imaging was performed. Figure 1B shows the M-mode ARF image that captures the response of the posterior and anterior surfaces of the cornea to ARF exposure. The horizontal line indicates the beginning of the push mode.

Figure 2 shows the continuous strain in the cornea during the prepush and push modes for the control (Figure 2A) and treated eye (Figure 2B) of one rabbit before and 1 through 4 weeks after treatment. The maximum observed strain was less than 1%. The coefficient of determination ($R^2$) values for the Voigt model fits ranged from 0.96 to 0.99, indicating that the data were a good fit to the model.

Figure 3 shows $E$ and η. One-way ANOVA showed no statistically significant change in $E$ or η in control eyes. The treated eyes showed significant alterations in $E$($F$ = 5.97; $P$ = .002) and η (F = 7.01; $P$ = .0007). The $t$ tests comparing eyes at 4 weeks after treatment to pretreated eyes showed that both of these parameters were significantly higher ($t$ = 3.47; $P$ = .006 for $E$; $t$ = 3.37; $P$ = .007 for η).

Figure 4 shows the stiffness factor for control and treated eyes before and 1 through 4 weeks after treatment. At 1 week after treatment, $E$ increased by a factor of 1.8. In the subsequent 3 weeks, this factor declined to 1.52, 1.49, and 1.30, respectively. One-way ANOVA showed no significant difference in the stiffness factor in control eyes. In the treated eyes, there was a statistically significant effect ($F$ = 5.11; $P$ = .004). At 4 weeks after treatment, the treated eyes were significantly stiffer than before treatment ($t$= 3.61; $P$ = .005). When the 2 rabbits that had their treatments interrupted were excluded from measurements (Figure 4B), the treated corneas were stiffer by a factor of 1.4 ($t$ = 6.66; $P$ = .0005) at 4 weeks after treatment.

Figure 5 shows the thickness of control and treated corneas before and 1 through 4 weeks after treatment. Although 1-way ANOVA showed significant changes in the thickness of treated corneas ($F$ = 5.59; $P$ = .002), at 4 weeks after treatment, the $t$ test showed that the cornea was not significantly thicker than before treatment. Average thickness and elasticity values were significantly correlated (Pearson $R$ = 0.94).

$T_{⅓}$ values calculated from sigmoidal fits and $\Delta T_{⅓}$ values at 4 weeks after treatment are shown in Table 1. These results confirm that the treatment was not effective in the 2 rabbits in which treatment was interrupted (rabbits 5 and 6) and are consistent with the in vivo stiffness factor measurements (Pearson $R$ = 0.75). The $t$ test showed that there was a significant difference in $T_{⅓}$ values between control and treated corneas ($t$ = 4.4; $P$ = .02) in the first 4 rabbits. Figure 6 presents the average changes in tissue cross-sectional areas as a function of temperature for rabbits 1 through 4 and their sigmoidal fits. The average $\Delta T_{⅓}$ between control and treated eyes was 1.07°C.

## Discussion

The aim of this study was to determine whether post–cross-linking corneal biomechanical changes could be shown noninvasively using ARF. We measured ARF-induced strain in the cornea and estimated tissue viscoelastic properties using the Voigt model. To our knowledge, we are the first group to demonstrate post–cross-linking biomechanical changes in the live cornea.

Previous studies using excised corneal strips in a microcomputer-controlled biomaterial tester have shown increases in corneal stiffness immediately after treatment by factors of 1.6

in rabbit corneas (n = 3)[20] and 1.8 and 4.5 in porcine (n = 20) and human (n = 5) corneas,[13] respectively. Two noninvasive techniques have been demonstrated recently on whole intact ex vivo porcine eyes, with measurements made immediately after cross-linking treatment.[17,19] The supersonic shear wave imaging technique[17] showed an increase in stiffness by a factor of 4.6. The Brillouin microscopy technique[19] showed statistically significant increases in stiffness in the anterior (factor of 1.07) and central (factor of 1.03) corneas (n = 6).

In this pilot study, we demonstrated increases in corneal stiffness using a noninvasive technique based on the generation of ARF-induced stress/strain after cross-linking in the rabbit eye. We found an increase in stiffness by a factor of 1.8 at 1 week after treatment. In the subsequent 3 weeks, this factor declined to 1.52, 1.49, and 1.30. Although there is a trend toward decreasing stiffness with time, we noticed that there was no such trend when 2 rabbits that had their treatments interrupted because of technical difficulties were excluded from measurements.

Improved biomechanical properties have been shown to be long term and stable (up to 8 months) in the ex vivo rabbit cornea.[20] Recently, long-term (up to 6 years) stability of cross-linking–treated keratoconic corneas has been demonstrated clinically based on visual acuity and corneal topography.[51] On the other hand, a recent report, in which corneal buttons obtained at transplant surgery were evaluated histologically, found decreasing effectiveness in edematous human cross-linking–treated corneas.[52]

Our results showed the cornea to be swollen immediately after treatment, stabilizing over the next 3 weeks to pretreatment values. Clinically, it is well known that the cornea becomes edematous after cross-linking therapy, resulting in blurry vision for up to 1 month.[53] Corneal edema resolves completely by 3 months after treatment.[53] For this reason, visual and structural tests are performed beginning at 1 month after cross-linking therapy. We found the cornea to be 15% thicker at 1 week after treatment, but the ARF-induced change in thickness ($\Delta T$) was 42% lower, causing an overall decrease in strain and thereby an increase in elasticity of 80% (a stiffness factor of 1.8). At 4 weeks after treatment, the corneal thickness had returned to the pretreatment value, and the 30% increase in elasticity was completely attributed to reduced strain. Thus, although our thickness and elasticity measurements were correlated, the higher stiffness cannot be attributed to corneal swelling. Longer-term assessment is required to demonstrate sustained improvement in stiffness in the treated cornea after its thickness has stabilized.

Corneal stiffening induced by cross-linking is depth dependent, with most of the effect occurring in the anterior third of the stroma.[4,19,54] In this study, we focused on whole-corneal strain and elasticity measurements. In the future, we plan to use speckle-tracking algorithms to monitor depth-dependent strain in the cornea using ARF. Future studies will also include correlation with ex vivo biomechanical measurements.

Ultrasound levels used in this study were compliant with US Food and Drug Administration guidelines for diagnostic ultrasound examinations of the eye, allowing clinical translation.

Although this study was conducted on anesthetized rabbits, the exposure duration of a few milliseconds will allow the technique to be readily applicable to awake human patients.

The capacity to measure corneal stiffness noninvasively offers a means for assessing the effectiveness and stability of cross-linking therapy in clinical patients and development of new and optimized cross-linking clinical protocols. In addition, this technique would be applicable in preclinical studies focused on formulation of new cross-linking agents and protocols, which would allow reduction of animal use by obviating the need to euthanize animals at various time points to determine biomechanical effects.

Noninvasive determination of corneal stiffness may also provide a new and independent parameter for early detection of keratoconus and other forms of corneal ectasia, in which corneal biomechanical integrity is compromised. At present, keratoconus is diagnosed on the basis of family history, corneal thickness, and surface topography.[55] Early detection of keratoconus offers the potential for early treatment by cross-linking to prevent disease progression.

Noninvasive corneal stiffness determination may also affect glaucoma management, since the accuracy of intraocular pressure measurement by applanation tonometry is affected by cornea biomechanical properties.[56] At present, corneal thickness is sometimes taken into account to correct intraocular pressure values obtained by applanation tonometry,[57] but the actual corneal stiffness may represent a superior means for accurate intraocular pressure assessment.

In conclusion, we have demonstrated increased corneal stiffness after riboflavin cross-linking in a rabbit model using a noninvasive technique based on ARF. Although more extensive and longer-term studies are necessary, our findings show that the technique may prove useful for monitoring of cross-linking and may have wider applications for assessment of corneal biomechanical properties.

## Acknowledgments

We thank David Paik, MD, and Quan Wen, MD, for help with thermal shrinkage temperature analysis, Jeffrey Ketterling, PhD, for help with developing the data acquisition software, Steve Trokel, MD, for the use of the Opto XLink corneal cross-linking system, and Jean-Marie Parel, PhD, for providing riboflavin for this study. This work was supported by an Endowment for Education and Research grant from the American Institute of Ultrasound in Medicine, National Institutes of Health grants EY019055, P30 EY019007, and an unrestricted grant to the Department of Ophthalmology of Columbia University from Research to Prevent Blindness.

## Abbreviations

| | |
|---|---|
| **ANOVA** | analysis of variance |
| **ARF** | acoustic radiation force |

## References

1. Rabinowitz YS. Keratoconus. Surv Ophthalmol. 1998; 42:297–319. [PubMed: 9493273]
2. Wollensak G, Spoerl E, Seiler T. Riboflavin/ultraviolet-a–induced collagen crosslinking for the treatment of keratoconus. Am J Ophthalmol. 2003; 135:620–627. [PubMed: 12719068]

3. Tomkins O, Garzozi HJ. Collagen cross-linking: strengthening the unstable cornea. Clin Ophthalmol. 2008; 2:863–867. [PubMed: 19668440]
4. Raiskup F, Spoerl E. Corneal crosslinking with riboflavin and ultraviolet A, I: principles. Ocul Surf. 2013; 11:65–74. [PubMed: 23583042]
5. Paik DC, Wen Q, Braunstein RE, Airiani S, Trokel SL. Initial studies using aliphatic B-nitro alcohols for therapeutic corneal cross-linking. Invest Ophthalmol Vis Sci. 2009; 50:1098–1105. [PubMed: 18836172]
6. Kissner A, Spoerl E, Jung R, Spekl K, Pillunat LE, Raiskup F. Pharmacological modification of the epithelial permeability by benzalkonium chloride in UVA/riboflavin corneal collagen cross-linking. Curr Eye Res. 2010; 35:715–721. [PubMed: 20673048]
7. Filippello M, Stagni E, O'Brart D. Transepithelial corneal collagen crosslinking: bilateral study. J Cataract Refract Surg. 2012; 38:283–291. [PubMed: 22104644]
8. Wollensak G, Wilsch M, Spoerl E, Seiler T. Collagen fiber diameter in the rabbit cornea after collagen crosslinking by riboflavin/UVA. Cornea. 2004; 23:503–507. [PubMed: 15220736]
9. Spoerl E, Wollensak G, Dittert DD, Seiler T. Thermomechanical behavior of collagen–cross-linked porcine cornea. Ophthalmologica. 2004; 218:136–140. [PubMed: 15004504]
10. Spoerl E, Wollensak G, Seiler T. Increased resistance of crosslinked cornea against enzymatic digestion. Curr Eye Res. 2004; 29:35–40. [PubMed: 15370365]
11. Beshtawi IM, O'Donnell C, Radhakrishnan H. Biomechanical properties of corneal tissue after ultraviolet-A–riboflavin crosslinking. J Cataract Refract Surg. 2013; 39:451–462. [PubMed: 23506922]
12. Spoerl E, Huhle M, Seiler T. Induction of cross-links in corneal tissue. Exp Eye Res. 1998; 66:97–103. [PubMed: 9533835]
13. Wollensak G, Spoerl E, Seiler T. Stress-strain measurements of human and porcine corneas after riboflavin-ultraviolet-A–induced cross-linking. J Cataract Refract Surg. 2003; 29:1780–1785. [PubMed: 14522301]
14. Wollensak G, Iomdina E. Biomechanical and histological changes after corneal crosslinking with and without epithelial debridement. J Cataract Refract Surg. 2009; 35:540–546. [PubMed: 19251149]
15. Wollensack G, Redl B. Gel electrophoretic analysis of corneal collagen after photodynamic cross-linking treatment. Cornea. 2008; 3:353–356.
16. Kling S, Remon L, Pérez-Escudero A, Merayo-Lloves J, Marcos S. Corneal biomechanical changes after collagen cross-linking from porcine eye inflation experiments. Invest Ophthalmol Vis Sci. 2010; 51:3961–3968. [PubMed: 20335615]
17. Tanter M, Touboul D, Gennisson JL, Bercoff J, Fink M. High-resolution quantitative imaging of cornea elasticity using supersonic shear imaging. IEEE Trans Med Imaging. 2009; 28:1881–1893. [PubMed: 19423431]
18. Dias J, Ziebarth NM. Effect of corneal crosslinking on anterior and posterior stromal elasticity assessed ex vivo by atomic force microscopy [abstract]. Invest Ophthalmol Vis Sci. 2012; 53(suppl):1523.
19. Scarcelli G, Kling S, Quijano E, Pineda R, Marcos S, Yun SH. Brillouin microscopy of collagen crosslinking: noncontact depth-dependent analysis of corneal elastic modulus. Invest Ophthalmol Vis Sci. 2013; 54:1418–1425. [PubMed: 23361513]
20. Wollensak G, Iomdina E. Long-term biomechanical properties of rabbit cornea after photodynamic collagen crosslinking. Acta Ophthalmol. 2009; 87:48–51. [PubMed: 18547280]
21. Raiskup-Wolf F, Hoyer A, Spoerl E, Pillunat LE. Collagen crosslinking with riboflavin and UVA-light in keratoconus: long-term results. J Cataract Refract Surg. 2008; 34:796–801. [PubMed: 18471635]
22. Vinciguerra P, Albé E, Trazza S, et al. Refractive, topographic, tomographic, and aberrometric analysis of keratoconic eyes undergoing corneal crosslinking. Ophthalmology. 2009; 116:369–378. [PubMed: 19167087]
23. Luce DA. Determining in vivo biomechanical properties of the cornea with an ocular response analyzer. J Cataract Refract Surg. 2005; 31:156–162. [PubMed: 15721708]

24. Goldich Y, Barkana Y, Morad Y, Hartstein M, Avni I, Zadok D. Can we measure corneal biomechanical changes after collagen cross-linking in eyes with keratoconus? A pilot study. Cornea. 2009; 28:498–502. [PubMed: 19421050]
25. Sedaghat M, Naderi M, Zarei-Ghanavati M. Biomechanical parameters of the cornea after collagen cross-linking measured by waveform analysis. J Cataract Refract Surg. 2010; 36:1728–1731. [PubMed: 20870120]
26. Albé E. Measuring corneal biomechanical properties in keratoconic eyes undergoing crosslinking. Cataract Refract Surg Today Eur. Jun.2008 :333–334.
27. Spoerl E, Terai N, Scholz F, Raiskup F, Pillunat LE. Detection of biomechanical changes after corneal cross-linking using Ocular Response Analyzer software. J Refract Surg. 2011; 27:452–457. [PubMed: 21243976]
28. Nyborg, W. Physical Acoustics. Academic Press Inc; New York, NY: 1965. Acoustic streaming; p. 265-331.
29. Torr G. The acoustic radiation force. Am J Phys. 1984; 52:402–408.
30. Nightingale K, Palmeri M, Nightingale R, Trahey G. On the feasibility of remote palpation using acoustic radiation force. J Acoust Soc Am. 2001; 110:625–634. [PubMed: 11508987]
31. Doherty JR, Trahey GE, Nightingale KR, Palmeri ML. Acoustic radiation force elasticity imaging in diagnostic ultrasound. IEEE Trans Ultrason Ferroelectr Freq Control. 2013; 60:685–701. [PubMed: 23549529]
32. Dymling SO, Persson HW, Hertz TG, Lindström K. A new ultrasonic method for fluid property measurements. Ultrasound Med Biol. 1991; 17:497–500. [PubMed: 1962351]
33. Viola F, Kramer MD, Lawrence MB, Oberhauser JP, Walker WF. Sonorheometry: a noncontact method for the dynamic assessment of thrombosis. Ann Biomed Eng. 2004; 32:696–705. [PubMed: 15171624]
34. Mauldin FW Jr, Haider MA, Loboa EG, et al. Monitored steady-state excitation and recovery (MSSER) radiation force imaging using viscoelastic models. IEEE Trans Ultrason Ferroelectr Freq Control. 2008; 55:1597–1610. [PubMed: 18986950]
35. Sarvazyan AP, Rudenko OV, Swanson SD, Fowlkes JB, Emelianov SY. Shear wave elasticity imaging: a new ultrasonic technology of medical diagnostics. Ultrasound Med Biol. 1998; 24:1419–1435. [PubMed: 10385964]
36. Bercoff J, Tanter M, Fink M. Supersonic shear imaging: a new technique for soft tissue elasticity mapping. IEEE Trans Ultrason Ferroelectr Freq Control. 2004; 51:396–409. [PubMed: 15139541]
37. Fatemi M, Greenleaf JF. Ultrasound-stimulated vibro-acoustic spectrography. Science. 1998; 280:82–85. [PubMed: 9525861]
38. Konofagou EE, Hynynen K. Localized harmonic motion imaging: theory, simulations and experiments. Ultrasound Med Biol. 2003; 29:1405–1413. [PubMed: 14597337]
39. Nightingale K, Soo MS, Nightingale R, Trahey G. Acoustic radiation force impulse imaging: in vivo demonstration of clinical feasibility. Ultrasound Med Biol. 2002; 28:227–235. [PubMed: 11937286]
40. Clevert DA, Stock K, Klein B, et al. Evaluation of acoustic radiation force impulse (ARFI) imaging and contrast-enhanced ultrasound in renal tumors of unknown etiology in comparison to histological findings. Clin Hemorheol Microcirc. 2009; 43:95–107. [PubMed: 19713604]
41. Lupsor M, Badea R, Stefanescu H, et al. Performance of a new elastographic method (ARFI technology) compared to unidimensional transient elastography in the noninvasive assessment of chronic hepatitis C: preliminary results. J Gastrointestin Liver Dis. 2009; 18:303–310. [PubMed: 19795024]
42. Friedrich-Rust M, Wunder K, Kriener S, et al. Liver fibrosis in viral hepatitis: noninvasive assessment with acoustic radiation force impulse imaging versus transient elastography. Radiology. 2009; 252:595–604. [PubMed: 19703889]
43. Frulio N, Trillaud H. Ultrasound elastography in liver. Diagn Interv Imaging. 2013; 94:515–534. [PubMed: 23623211]
44. Silverman RH, Urs R, Lloyd HO. Effect of ultrasound radiation force on the choroid. Invest Ophthalmol Vis Sci. 2013; 54:103–109. [PubMed: 23211817]

45. Viola F, Walker W. A spline-based algorithm for continuous time-delay estimation using sampled data. IEEE Trans Ultrason Ferroelectr Freq Control. 2005; 52:80–93. [PubMed: 15742564]
46. Paik DC, Wen Q, Airiani S, Braunstein RE, Trokel SL. Aliphatic β-nitro alcohols for non-enzymatic collagen cross-linking of scleral tissue. Exp Eye Res. 2008; 87:279–285. [PubMed: 18616942]
47. Ruijgrok JM, de Wijn JR, Boon ME. Glutaraldehyde crosslinking of collagen: effects of time, temperature, concentration and presoaking as measured by shrinkage temperature. Clin Mater. 1994; 7:23–27. [PubMed: 10150174]
48. Moore MA, Chen WM, Phillips RE, Bohachevsky IK, McIlroy BK. Shrinkage temperature versus protein extraction as a measure of stabilization of photooxidized tissue. J Biomed Mater Res. 1996; 32:209–214. [PubMed: 8884497]
49. Fathima NN, Madhan B, Rao JR, Nair BU, Ramasami T. Interaction of aldehydes with collagen: effect on thermal, enzymatic and conformational stability. Int J Biol Macromol. 2004; 34:241–247. [PubMed: 15374680]
50. Silverman RS, Patel MS, Gal O, et al. Effect of corneal hydration on ultrasound velocity and backscatter. Ultrasound Med Biol. 2009; 35:839–846. [PubMed: 19195769]
51. O'Brart DP, Kwong TQ, Patel P, McDonald RJ, O'Brart NA. Long-term follow-up of riboflavin/ultraviolet A (370 nm) corneal collagen cross-linking to halt the progression of keratoconus. Br J Ophthalmol. 2013; 97:433–437. [PubMed: 23385632]
52. Botto's KM, Hofling-Lima AL, Barbosa MC, et al. Effect of collagen cross-linking in stromal fibril organization in edematous human corneas. Cornea. 2010; 29:789–793. [PubMed: 20489599]
53. Dahl BJ, Spotts E, Truong JQ. Corneal collagen cross-linking: an introduction and literature review. Optometry. 2012; 83:33–42. [PubMed: 22153823]
54. Kohlhaas M, Spoerl E, Schilde T, Unger G, Wittig C, Pillunat LE. Biomechanical evidence of the distribution of cross-links in corneas treated with riboflavin and ultraviolet A light. J Cataract Refract Surg. 2006; 32:279–283. [PubMed: 16565005]
55. Gatinel D, Saad A. The challenges of the detection of subclinical keratoconus at its earliest stage. Int J Keratoco Ectatic Corneal Dis. 2012; 1:36–43.
56. Costin BR, Fleming GP, Weber PA, Mahmoud AM, Roberts CJ. Corneal biomechanical properties affect Goldmann applanation tonometry in primary open-angle glaucoma. J Glaucoma. 2014; 23:69–74. [PubMed: 23603825]
57. Whitacre MM, Stein RA, Hassanein K. The effect of corneal thickness on applanation tonometry. Am J Ophthalmol. 1993; 115:592–596. [PubMed: 8488910]

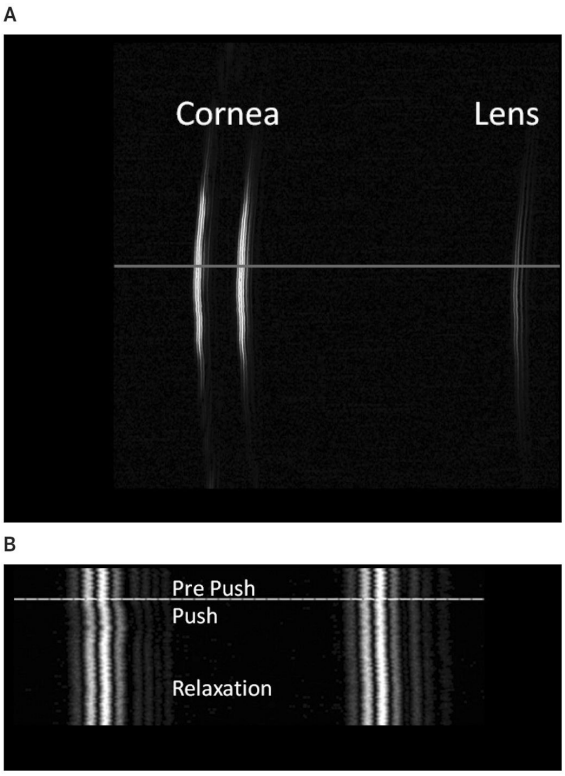


**Figure 1.**

**A**, B-mode image of a rabbit cornea and the anterior surface of the lens. Acoustic radiation force imaging was performed on 3 spots in the central cornea. **B**, Acoustic radiation force image, retaining phase information, along one line of sight (horizontal line in **A**) showing displacement of the cornea. The horizontal line in **B** indicates the beginning of the ARF application.

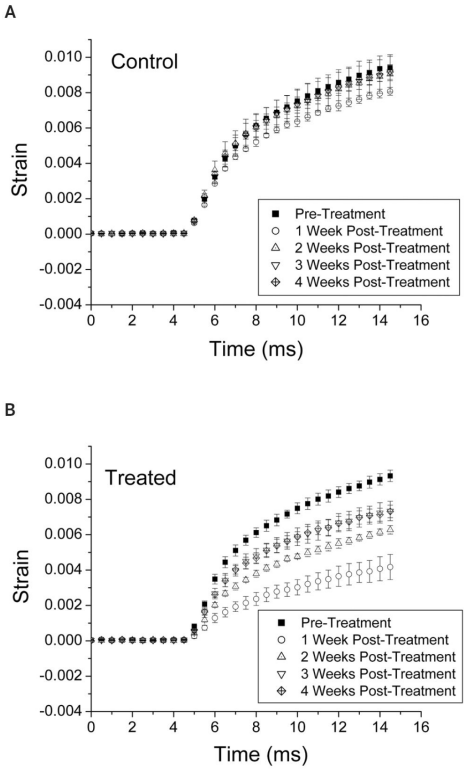


**Figure 2.**

Acoustic radiation force–induced strain ± 1 SD before and 1 through 4 weeks after treatment in the control eye (**A**) and treated eye (**B**) of one rabbit. Acoustic radiation force was applied for a total duration of 8 milliseconds for 80% of the time beginning at 5 milliseconds and ending at 15 milliseconds. The maximum observed strain was less than 1%. Decreased strain in the treated eye is indicative of increased stiffness.

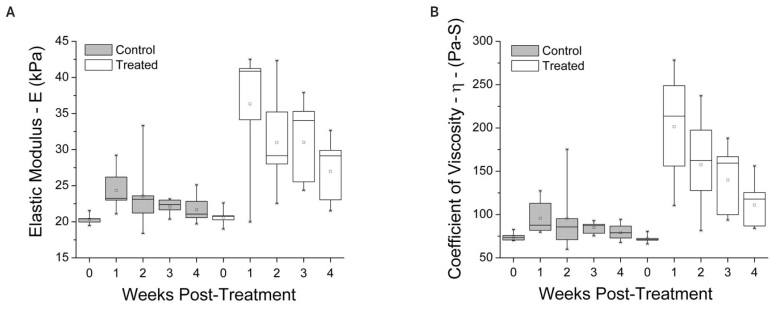


**Figure 3.**

Elastic modulus (*E*; **A**) and coefficient of viscosity (η; **B**) values for control and treated eyes before and 1 through 4 weeks after treatment. One-way ANOVA showed no significant differences in the control eyes. The treated eyes were significantly different ($F = 5.97$; $P = .002$ for *E*; $F = 7.01$; $P = .0007$ for η). At 4 weeks after treatment, *E* and η were significantly higher in the treated corneas ($t = 3.47$; $P = .006$ for *E*; $t = 3.37$; $P = .007$ for η).

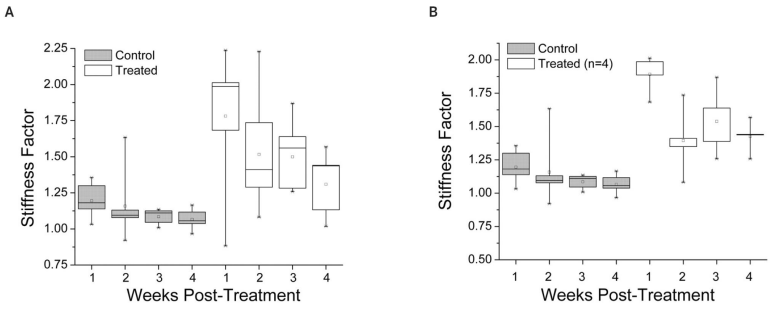


**Figure 4.**

**A**, Stiffness factors for all control and treated eyes (ratio of *E* at 1–4 weeks after treatment to *E* before treatment). At 4 weeks after treatment, the treated corneas were stiffer by a factor of 1.3 ($t = 3.61$; $P = .005$). **B**, Stiffness factors when 2 rabbits that had their treatments interrupted because of technical difficulties were excluded from measurements. At 4 weeks after treatment, the treated corneas in 4 rabbits were stiffer by a factor of 1.4 ($t = 6.66$; $P = .0005$). There was no trend toward decreasing stiffness with time from week 2 to week 4.

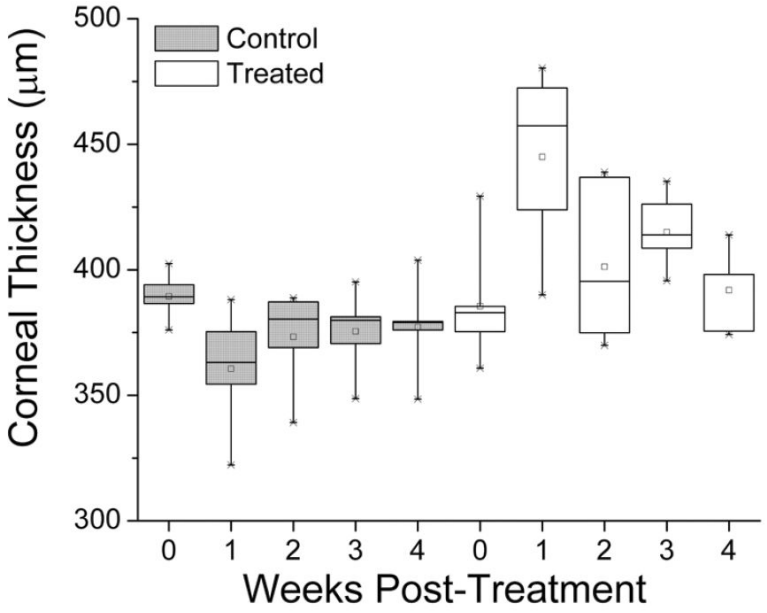


**Figure 5.**

Corneal thickness of control and treated eyes before and 1 through 4 weeks after treatment. Although 1-way ANOVA showed significant changes in thickness after treatment ($F = 5.59$; $P = .002$), at 4 weeks after treatment, the corneal thickness was not significantly thicker than before treatment.

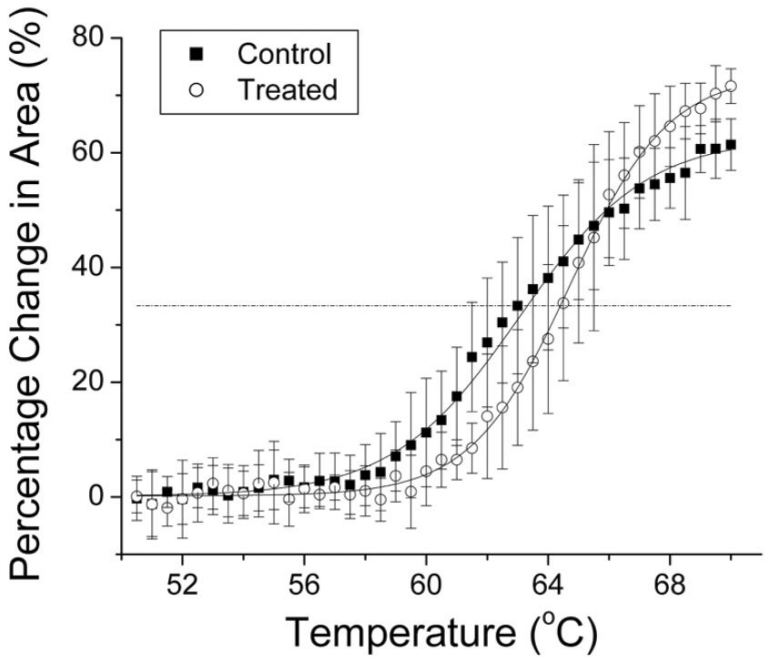


**Figure 6.**

Average percent change in ex vivo corneal tissue strip cross-sectional areas in control and treated eyes of rabbits 1 through 4. $\Delta T_{1/3}$ was calculated from sigmoidal fits to be 1.07°C. The horizontal line represents $T_{1/3}$.

## Table 1

$T_{1/3}$ Values Calculated From Sigmoidal Fits, Differences in $T_{1/3}$ Values Between Control and Treated Corneas, and Stiffness Factors in Treated Corneas at 4 Weeks After Treatment.

| Rabbit | $T_{1/3}$, °C (Treated) | $T_{1/3}$, °C (Control) | $T_{1/3}$, °C (Treated – (Control) | Stiffness Factor 4 wk After Treatment (Treated) |
|---|---|---|---|---|
| 1 | 63.22 | 61.57 | 1.65 | 1.44 |
| 2 | 63.71 | 62.33 | 1.38 | 1.57 |
| 3 | 65.36 | 64.71 | 0.65 | 1.26 |
| 4 | 65.39 | 64.68 | 0.71 | 1.44 |
| 5 | 64.08 | 63.88 | 0.20 | 1.02 |
| 6 | 63.66 | 64.63 | −0.97 | 1.13 |